

RESEARCH

Open Access



Spatial pattern and driving factors of biomass carbon density for natural and planted coniferous forests in mountainous terrain, eastern Loess Plateau of China

Lina Sun, Mengben Wang and Xiaohui Fan*

Abstract

Background: Understanding the spatial pattern and driving factors of forest carbon density in mountainous terrain is of great importance for monitoring forest carbon in support of sustainable forest management for mitigating climate change.

Methods: We collected the forest inventory data in 2015 in Shanxi Province, eastern Loess Plateau of China, to explore the spatial pattern and driving factors of biomass carbon density (BCD) for natural and planted coniferous forests using Anselin Local Moran's I, Local Getis-Ord G^* and semivariogram analyses, and multi-group structural equation modeling, respectively.

Results: The result of spatial pattern of BCDs for natural forests showed that the BCD was generally higher in the north but lower in the south of Shanxi. The spatial pattern for planted forests was substantially different from that for natural forests. The results of multi-group SEM suggested that elevation (or temperature as the alternative factor of elevation) and stand age were important driving factors of BCD for these two forest types. Compared with other factors, the effects of latitude and elevation on BCD showed much greater difference between these two forest types. The difference in indirect effect of latitude (mainly through affecting elevation and stand age) between natural and planted forests was to some extent a reflection of the difference between the spatial patterns of BCDs for natural and planted forests in Shanxi.

Conclusions: The natural coniferous forests had a higher biomass carbon density, a stronger spatial dependency of biomass carbon density relative to planted coniferous forests in Shanxi. Elevation was the most important driving factor, and the effect on biomass carbon density was stronger for natural than planted coniferous forests. Besides, latitude presented only indirect effect on it for the two forest types.

Keywords: Spatial pattern, Spatial heterogeneity, Multi-group structural equation modeling, Stand age, Elevation, Mountainous terrain

* Correspondence: fanxiaohui@sxu.edu.cn

Institute of Loess Plateau, Shanxi University, Wucheng Road 92, Taiyuan 030006, China

Introduction

The role of forests as terrestrial sinks of atmospheric carbon dioxide has received increasing attention since the late 1990s (FAO 2010, 2015). Assessment of carbon density and storage of forests has been a focus in recent years (Fang 2001; Pan et al. 2011). Mountain forests account for 28% of the total global forest area (Price et al. 2000), and are considered to be important terrestrial sinks of carbon dioxide (Chang et al. 2015; Zald et al. 2016). Understanding the spatial patterns and driving factors of forest carbon density in mountainous terrain is of great importance for monitoring forest carbon in support of sustainable forest management for mitigating climate change (Zald et al. 2016).

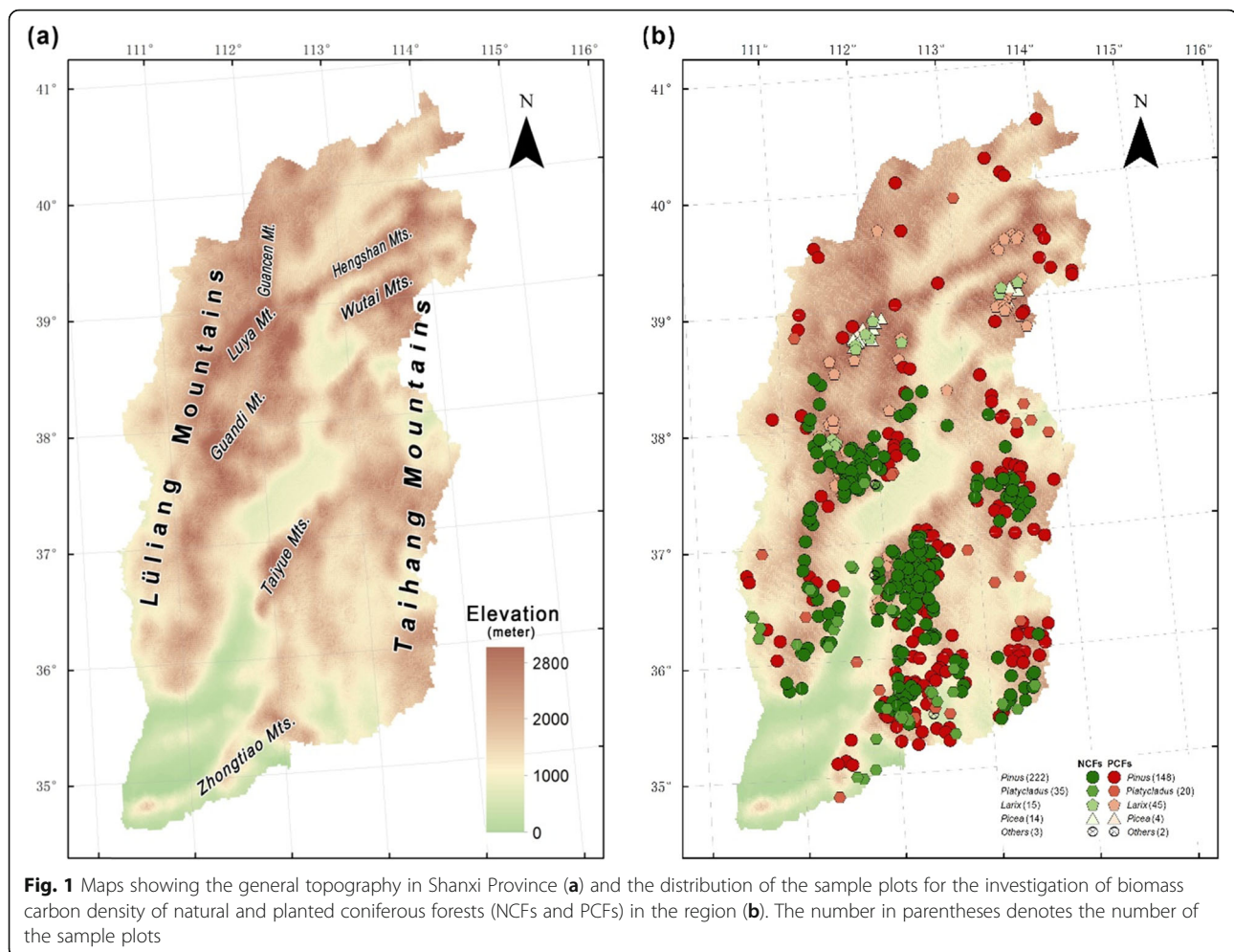
The spatial pattern information of forest carbon density can play an important role in evaluating carbon sequestration potentials and forest management (Fu et al. 2015; Lin et al. 2017; Verkerk et al. 2019). Ren et al. (2013) examined the spatial pattern of carbon density in forest ecosystems in Guangdong Province, and found that the spatial distribution of forest carbon density was uneven, and it was a reflection of the difference in forest management and economic and social development. Fu et al. (2014) observed a clear spatial pattern of forest litter carbon density in Zhejiang Province using Anselin Local Moran's I and geostatistical interpolation. A similar result was found for forest biomass carbon density in the same province (Fu et al. 2015). Using the same methods, Dai et al. (2018) further found that the forest carbon density decreased from southwest to northeast in Zhejiang Province, roughly in line with the topographic feature across this province. Using Anselin Local Moran's I, Local Getis-Ord G^* and geostatistical interpolation, Lin et al. (2017) analyzed the spatial variability of forest carbon density in Jiangle County, Fujian Province. However, little attempt has been made to compare the spatial patterns of carbon densities between natural and planted forests (Wang et al. 2018a).

Forest carbon density and their spatial patterns in mountainous terrain may be the result of complex interaction among various driving factors. Temperature and precipitation are two critical climatic factors driving biomass carbon density. For example, structural equation modeling (SEM) revealed that forest biomass carbon density were primarily controlled by climate factors, and increased with rising temperature and precipitation along the north-south transect of eastern China (Wen and He 2016); while multi-group SEM showed that mean annual temperature had negative indirect effect on carbon density in old-growth tropical forests across the globe (Durán et al. 2015). Meanwhile, previous studies have revealed that stand age and canopy coverage are important driving factors of forest carbon density. For instance, Xu et al. (2010) reported that forest age had

significant effect on biomass carbon density for most forest types in China. The average above-ground biomass carbon density of mature forests increased with stand age for the forests younger than 450 years (Liu et al. 2014); while the biomass carbon density of ponderosa pine forest increases rapidly until 150–200 years (Law et al. 2003). The SEM indicated that canopy coverage and stand age were the most important driving factors of biomass carbon density in subtropical forests (Xu et al. 2018a, 2018b). Moreover, the effect of elevation on forest carbon density has attracted great attention, especially in mountainous areas. For example, Gairola et al. (2011) found a significant positive relationship of forest biomass carbon density with elevation in moist temperate valley slopes of the Garhwal Himalaya (India). Liu and Nan (2018) reported a positive relationship between carbon density and elevation for three natural coniferous forests in the Guandi Mountain, Shanxi Province. In addition, as another important geographical factor, latitude may have indirect effect on forest biomass carbon density by affecting plant growth and productivity through temperature and precipitation effects. It was found that the forest biomass carbon density decreased with increasing latitude along the north-south transect of eastern China (Wen and He 2016); while the biomass carbon density of Moso bamboo forests linearly increased with latitude (Xu et al. 2018a, 2018b).

Shanxi Province is a mountainous terrain in north China, characterized by six mountain ranges, namely the Hengshan and Wutai Mountains in the north, the Zhongtiao Mountains in the south, the Lüliang Mountains in the west, the Taihang Mountains in the east, and the Taiyue Mountains at the center (Fig. 1a). Coniferous forests are widely distributed in the province, prominently in the high mountains. In the past few decades, China has launched a series of large-scale afforestation and forest protection programs, including the Three-North Shelter Forest Program since 1978, the Program for Conversion of Cropland into Forests since 1999, and the Natural Forest Protection Program since 2000. With the implementation of these national projects, the areas of natural and planted coniferous forests (NCFs and PCFs, respectively), and their contributions to regional carbon stocks may have changed substantially in this region.

Previous studies have examined the carbon density and carbon stocks of *Pinus tabulaeformis* forest in Shanxi on a local (Sun 2011; Cheng et al. 2012; Chi et al. 2014) or provincial scale (Wang et al. 2014a). Recently, Liu and Nan (2018) examined the carbon stocks of three natural coniferous forests (*Larix principis-rupprechtii* forest, *Picea meyerii* forest and *Pinus tabulaeformis* forest) along an altitudinal gradient from 1200 to 2700 m in the Guandi Mountain. Wang et al. (2018a) analyzed the



spatial patterns of carbon densities of natural and planted forests in the Lüliang Mountains. An integrated study of carbon density of coniferous forests is urgently needed for a proper evaluation of the current capacity of carbon sequestration of natural versus planted coniferous forests and for a better understanding of how various factors affect the carbon density of natural versus planted coniferous forests in the mountainous region.

Within this context, the main objectives of this study were to quantify the biomass carbon densities and stocks of natural and planted coniferous forests in Shanxi Province, China, and to explore the spatial patterns and driving factors of biomass carbon density of natural and planted coniferous forests in the mountainous terrain. We first used the national forest inventory data in 2015 to quantify the biomass carbon densities based on the method of biomass expansion factor. We then characterized the spatial patterns of biomass carbon density of natural and planted coniferous forests using Anselin Local Moran's I, Local Getis-Ord G^* and semivariogram analyses. Finally, we used multi-group structural equation modeling to evaluate relative importance of driving

factors selected in explaining variations of biomass carbon density, to estimate the direct and indirect effects of each driving factor, and to reveal the similarities and differences between the models for natural and planted coniferous forests.

Materials and methods

Study region

Shanxi Province is located in the middle reach of the Yellow River, and the east of the Loess Plateau in north China, at $34^{\circ}34' - 40^{\circ}43' N$ and $110^{\circ}14' - 114^{\circ}33' E$, with a total area of $156,271 \text{ km}^2$ (Fig. 1a). As a mountainous plateau, the mountains and hills make up 80.3% of the province's land area (Fan and Wang 2011). Climatically, Shanxi belongs to the temperate monsoon climate zone (Guo et al. 2015) and is influenced by the summer and winter monsoons, with a hot and wet summer and a dry cold winter. The total area of forests is about $32,100 \text{ km}^2$, accounting for 20.05% of the province's land area. Coniferous forests account for 43% of all the forests in the province (Editorial Board of Forests in Shanxi 1992; Ma 2001).

Data collection and preprocessing

Forest inventory data

The data from a total of 508 field sample plots were used in this study. Of all the plots from the 9th national forest inventory data in 2015, 289 and 219 are natural and planted coniferous forests plots, respectively (Table 1, Fig. 1b). The permanent plots (each with an area of 667 m²) were established systematically based on a 4 km × 4 km grid (Xiao 2005). The data collected in each plot included forest origin, forest type, forest stand factors (stand age, age group, diameter at breast height of 1.3 m (DBH), tree height and forest coverage), and geographic location (latitude, longitude and elevation). For trees with DBH ≥ 5 cm, their DBH were recorded. A total of 12 dominant coniferous tree species were identified over the study region. According to the dominant species, all the natural (planted) coniferous forests were classified into five categories: *Pinus*, *Platycladus*, *Larix*, *Picea* and other forests (Fig. 1b).

For each forest plot (each forest stand), the carbon density (CD) (Mg·ha⁻¹) of living trees was estimated using the biomass expansion factor (BEF) method (Wang et al. 2018a):

$$CD = (V \times WD \times BEF) \times (1 + R) \times CF \quad (1)$$

where V is the volume of biomass (m³·ha⁻¹), i.e., the sum of the above-ground trunk volumes of individual living trees; WD is the wood density (Mg·m⁻³), BEF is the biomass expansion factor, R is the root-shoot ratio, and CF represents carbon content in oven-dried

biomass, i.e., the ratio of carbon (Mg) to oven-dried biomass (Mg). The V for individual trees was calculated using the diameter at breast height of 1.3 m and the height of each tree based on the formula for each tree species (Wang et al. 2018b).

In this study, the biomass carbon density (BCD, Mg·ha⁻¹) represented only the carbon density of living trees, and did not include that from shrubs, herbs, litter, and soil. The mean BCD of each forest type was estimated by dividing the sum of biomass carbon densities of the forest plots by the number of the forest plots for the forest type. The total biomass carbon stock (Mg) for each forest type was estimated by multiplying the mean biomass carbon density by the area of the forest type, which was approximated by multiplying the representative area (4 km × 4 km) of a sample plot by the number of the forest plots.

Climate data

The data of annual mean temperature (TEMP) and mean annual precipitation (PRCP) for the period 1981–2010 at the 61 meteorological stations were obtained from the meteorological database of the scientific data platform of Shanxi Province. The TEMP (PRCP) for each sample plot was computed by interpolation of the measurements (1981–2010 means) of the 61 stations using regression-kriging interpolation method (Lamsal et al. 2011; Plouffe et al. 2015), which combined regression of the climatic variable on topography variables (slope degree, slope aspect and slope position) with kriging of the regression residuals (Eldeiry and Garcia

Table 1 Descriptive statistics of stand age, stand coverage, elevation, latitude, annual mean temperature and annual precipitation for natural and planted coniferous forests in the study region

Forest type	AGE (year)		COV (%)		ELE (km)		LAT (°)		TEMP (°C)		PRCP (mm)		N
	mean	Range	mean	Range	mean	Range	mean	Range	mean	Range	mean	Range	
Natural coniferous forests													
<i>Pinus</i>	54	14–95	55	20–90	1.428	0.950–1.940	36.81	35.41–38.44	6.7	3.0–10.5	500.8	406.3–599.3	222
<i>Platycladus</i>	48	25–85	50	20–85	1.018	0.483–1.600	36.01	34.97–37.51	9.5	5.4–13.3	529.2	425.6–607.8	35
<i>Larix</i>	62	17–91	54	29–75	2.235	1.870–2.500	38.47	37.84–39.13	1.7	–0.5–4.2	476	430.3–558.2	15
<i>Picea</i>	65	26–86	65	20–97	2.305	1.862–2.560	38.76	37.89–39.09	1.1	–0.5–3.7	468.1	446.5–569.8	14
others	27	9–55	38	22–62	1.509	1.260–1.647	37.99	36.72–39.75	5.7	3.6–8.1	433.3	395.3–478.9	3
All	54	9–95	55	20–97	1.464	0.483–2.560	36.91	34.97–39.75	6.5	–0.5–13.3	500.7	395.3–607.8	289
Planted coniferous forests													
<i>Pinus</i>	31	5–61	59	20–91	1.306	0.476–2.100	36.98	35.10–40.50	7.3	2.7–11.5	510.8	374.2–604.0	148
<i>Platycladus</i>	13	5–42	33	20–90	0.916	0.400–1.300	36.76	34.83–39.90	9.8	6.2–13.6	507.3	374.4–581.7	20
<i>Larix</i>	26	8–60	57	20–95	1.893	1.260–2.383	38.42	36.43–39.67	3.2	–0.1–7.8	489.7	404.5–620.9	45
<i>Picea</i>	35	15–47	69	30–92	2.209	1.717–2.410	38.89	38.79–38.97	1.4	0.4–3.4	495.7	452.5–619.8	4
others	11	6–15	23	20–25	1.067	0.697–1.436	37.14	35.49–38.80	8.7	6.1–11.3	504.8	430.8–578.8	2
All	28	5–61	56	20–95	1.405	0.400–2.410	37.29	34.83–40.50	6.6	–0.1–13.6	505.8	374.2–620.9	219

AGE, stand age; COV, stand coverage; ELE, elevation; LAT, latitude; TEMP, annual mean temperature; and PRCP, annual precipitation. N, number of sample plots

2010). Similar as in the previous study (Wang et al. 2018a), the TEMP of each plot from the interpolation was further corrected according to the difference between the plot elevation and the interpolated elevation using the temperature lapse rate of 4.89 °C·km⁻¹ as the correction factor (Wang et al. 2014b).

Data analysis

Statistical analyses

The dataset of mean BCDs for each forest type met the normal distribution and passed the homogeneity of variances test, and then One-way ANOVA with Duncan’s multiple tests was used to examine the difference in mean BCD between/among forest types.

Spatial pattern analyses

Anselin Local Moran’s I, Local Getis-Ord G* and semi-variogram analyses were used to investigate the spatial patterns of forest BCDs from different aspects. Anselin Local Moran’s I can be used to identify spatial clusters and outliers (Fu et al. 2015). The significant positive values of the index show clusters that represent positive spatial autocorrelation; the significant negative values of this index show outliers that represent negative spatial autocorrelation; and the “not significant” values represent no spatial autocorrelation. The clusters consist of high-high clusters (high values in a high value neighborhood) and low-low clusters (low values in a low value neighborhood); and the outliers include high-low outlier (a high value surrounded by low values) and low-high outlier (a low value surrounded by high values) (Fu et al. 2015; Lin et al. 2017; Dai et al. 2018). The statistic of Anselin Local Moran’s I can be expressed as:

$$I_i = \frac{x_i - \bar{X}}{S_i^2} \sum_{j=1, j \neq i}^n w_{i,j} (x_j - \bar{X}) \tag{2}$$

$$S_i^2 = \frac{\sum_{j=1, j \neq i}^n (x_j - \bar{X})^2}{n-1} \tag{3}$$

where x_i and x_j are the values of attribute for observations i and j , respectively, \bar{X} is the mean of the corresponding values of the attribute, $w_{i,j}$ is the spatial weight between observations i and j , which can be defined as the fixed distance, which was obtained based on the largest global Moran’s I value, indicating the strongest spatial autocorrelation of carbon density (Fu et al. 2014). The $w_{i,j}$ is given the same weight within the distance, while those outside the distance band are given the weight of 0. The symbol of n is the total number of observations.

Meantime, Local Getis-Ord G* can be used to detect spatial hot spots and cold spots that represent clusters of

similar values that are significantly larger and smaller than the mean, respectively. There is a Z score for each target value in the test. For statistically significant positive Z scores, the larger the Z score is, the more intense the clustering of high values (hot spot). For statistically significant negative Z scores, the smaller the Z score is, the more intense the clustering of low values (cold spot). The “not significant” positive or negative Z scores represent no spatial autocorrelation (Manepalli et al. 2011). Getis-Ord Gi* can be described as:

$$G_i^* = \frac{\sum_{j=1}^n w_{i,j} x_j - \bar{X} \sum_{j=1}^n w_{i,j}}{\sqrt{\frac{\sum_{j=1}^n x_j^2}{n} - (\bar{X})^2} \sqrt{\frac{n \sum_{j=1}^n w_{i,j}^2 - \left(\sum_{j=1}^n w_{i,j}\right)^2}{n-1}}} \tag{4}$$

where $x_i, x_j, \bar{X}, w_{i,j}$, and n are the same as in Eq. 2.

Anselin Local Moran’s I can be used to study a certain spatial regularity, while Local Getis-Ord Gi* enables differentiation between clusters of similar values that are high or low relative to the mean, thus aiding in the detection of unusual events (Lin et al. 2017). The two indicators of exploring spatial autocorrelation were carried out using the modules of Cluster and Outlier Analysis (Anselin Local Moran’s I) and Hot Spot Analysis (Getis-Ord Gi*) of Spatial Statistics Toolbox within software ARCGIS 10.2.

Furthermore, semivariogram analysis was used to explore the spatial heterogeneity of forest biomass carbon density. Semivariogram analysis is a useful tool for analysis and interpretation of spatial data in ecology (Robertson 1987; Rossi et al. 1992) and has been used in quantification of spatial heterogeneity of forest carbon density (Wang et al. 2018a). We performed this analysis based on the standard principles of semivariogram model fitting in geostatistics (Wang 1999) using GS+ 9.0 Geostatistics Software (Gamma Design Software, LLC). This analysis was not only performed for the data of BCD but also for the data from the cluster and outlier analysis, and hot spot analysis to examine further the spatial heterogeneity of BCD of natural versus planted forests over the study region.

Multi-group SEM

Multi-group SEM was used to compare the direct and indirect effects of the main driving factors on BCD between NCFs and PCFs. Before constructing the multi-group SEM model, we tested the collinearity of the driving factors, and eliminated annual mean temperature (TEMP) from further analysis (see Annex 1 of Additional file 1).

We began with the construction of a priori model for the multi-group SEM procedure. The priori model was

constructed to include all hypothesized causal relationships between BCD and potential driving factors based on the known effects of driving factors and the relationships among driving factors of forest growth and biomass accumulation (Bollen 1989; Shipley 2004; Xu et al. 2018a, 2018b). As shown in Annex 2a of Additional file 1, five driving factors were included in the priori model: stand age, stand coverage, mean annual precipitation, latitude, and elevation.

The second step was to find a good-fitting structural equation model (Grace et al. 2010) to the data of all coniferous forests based on the priori model. We compared the actual and estimated covariance matrices to determine whether the model was acceptable using the chi-square (χ^2) test, comparative fit index (CFI) and root square mean error of approximation (RMSEA). If the model is not acceptable, the model is further revised by removing or adding a connection between variables according to the modification indices and corresponding parameter changes expected. The process is performed continuously until finding a good-fitting model (see Annex 2b of Additional file 1).

The final step was to fit a multi-group SEM model for NCFs and PCFs. (1) The most constrained multi-group SEM was first performed, for which individual path coefficients were forced to be equal between groups (Shipley 2004). If the multi-group model was rejected ($P < 0.05$), indicating that at least one path is not equal between groups (Shipley 2004), and further analysis will be performed. Otherwise, if it was acceptable ($P > 0.05$), indicating that there is no any difference between groups; and no further analysis will be carried out. (2) By taking a full free multi-group model as a starting point, fitting a series of nested models to find which paths were equal

or which paths differ across groups. For the nested models, only one path of the model could be constrained to be equal between groups at a time (Table 2). The difference in the maximum likelihood χ^2 statistics between models before and after adding an equal constrained path was used to test if this change is acceptable. (3) Multi-group SEM was fitted by constraining those path coefficients acceptable across groups. The SEM and multi-group SEM were implemented using the R version 3.4.4 and lavaan package version 0.6–3 (Rosseel 2012).

Results

Biomass carbon density and storage

The mean BCD of NCFs was significantly larger than that of PCFs (26.46 Mg·ha⁻¹ versus 18.69 Mg·ha⁻¹), with an average BCD of 23.07 Mg·ha⁻¹ for all coniferous forests (Table 3). A significant difference was detected among the average BCDs of the four main types of forests (Table 3). For the four main types of forests: *Pinus*, *Platycladus*, *Larix* and *Picea* forests, the mean BCD for natural forests was significantly larger than that for planted forests for the first three types of forests, but not for the last one. The average BCD of natural and planted forests was the largest for *Picea* forests, followed by *Larix* and *Pinus* forests, and it was the smallest for *Platycladus* forests.

The BCD varied with forests age. For all the natural or planted coniferous forests, the BCD increased from young to near-mature forests, while it slightly decreased for mature forests (there was no over-mature forests) relative to near-mature forests (Table 4). Although the average BCD of NCFs appeared higher than that of PCFs for every age group, a significant difference was only detected for young and half-mature age groups (Table 4).

Table 2 Multi-group comparison of path coefficients between natural and planted coniferous forests. A non-significant value, highlighted in bold, indicates that the path contribution to the model is equal between forest types

Free parameter between-groups was constrained	ML χ^2	Δ ML χ^2	P-value
None	9.688		
path from LAT to PRCP	18.075	8.434	0.004
path from LAT to ELE	45.411	35.723	0.000
path from COV to BCD	9.726	0.038	0.846
path from PRCP to BCD	10.115	0.427	0.514
path from ELE to BCD	13.816	4.127	0.042
path from LAT to AGE	16.807	7.101	0.008
path from ELE to AGE	9.844	0.153	0.696
path from AGE to COV	14.844	5.233	0.022
path from AGE to BCD	9.854	0.166	0.684
path from PRCP to COV	9.707	0.024	0.876

The first row shows the maximum likelihood χ^2 estimates (ML χ^2) when all parameters are free. The remaining rows show the result by constraining one parameter at a time. The difference between the fully free model and the rest is given as Δ ML χ^2 , and the P-value indicates the probability that the constraint of that parameter changes the model. Bonferroni-corrected P-value threshold, $0.05/13 = 0.0038$. BCD, biomass carbon density; AGE, stand age; COV, stand coverage; LAT, latitude; ELE, elevation; PRCP, mean annual precipitation

Table 3 Mean biomass carbon density (Mean BCD) and biomass carbon storage (BCS) of natural, planted and all coniferous forests in the study region

Forest type	Mean BCD (Mg·ha ⁻¹)			BCS (10 ⁴ Mg)		
	Natural	Planted	All	Natural	Planted	All
<i>Pinus</i> ^a	23.36 _a	17.02 _a	20.83 _a	819.18	397.99	1217.17
<i>Platyclusus</i> ^a	11.74 _b	1.95 _b	8.07 _b	64.91	6.46	71.37
<i>Larix</i> ^a	52.83 _c	27.67 _a	33.96 _c	125.18	196.7	321.88
<i>Picea</i>	85.76 _d	67.48 _c	81.70 _d	189.67	42.64	232.31
others	15.37	1.69	10.81	4.88	0.27	5.15
Mean ^a /Total	26.46	18.69	23.07	1203.82	644.06	1847.88

(1)^a There is a significant difference between the mean BCDs of natural and planted forests ($P < 0.05$). (2) Within a column, means followed by different letters are significantly different ($P < 0.05$)

It was also observed that the total amount of biomass carbon storage (BCS) for all the coniferous forests was 18.48×10^6 Mg (Table 4). The BCS of NCFs was nearly two times that of PCFs (12.04×10^6 Mg versus 6.44×10^6 Mg), and accounted for 65.1% and 34.9% of the total BCS, respectively. For the four main types of forests, the *Pinus* forests had the largest contribution (65.9%) to the total BCS, followed by *Larix* and *Picea* forests (17.4% and 12.6%, respectively), and *Platyclusus* forests had the smallest contribution (3.9%). Of the total BCS, half-mature forests accounted for 54.6%, and near-mature, young, and mature forests 28.6%, 10.5% and 6.3%, respectively (Annex 4 of Additional file 1).

Spatial autocorrelation and heterogeneity of biomass carbon density

Anselin Local Moran's I analysis showed that the number of the high-high clusters of BCD for NCFs was more than twice that for PCFs (Fig. 2). The high-high cluster areas for the NCFs were identified in the Wutai, Guancen and Guandi Mountains. In contrast, the high-high cluster areas for the PCFs were observed in the Hengshan, Wutai, Guancen and Luya Mountains. The low-low clusters for NCFs were mainly distributed in the

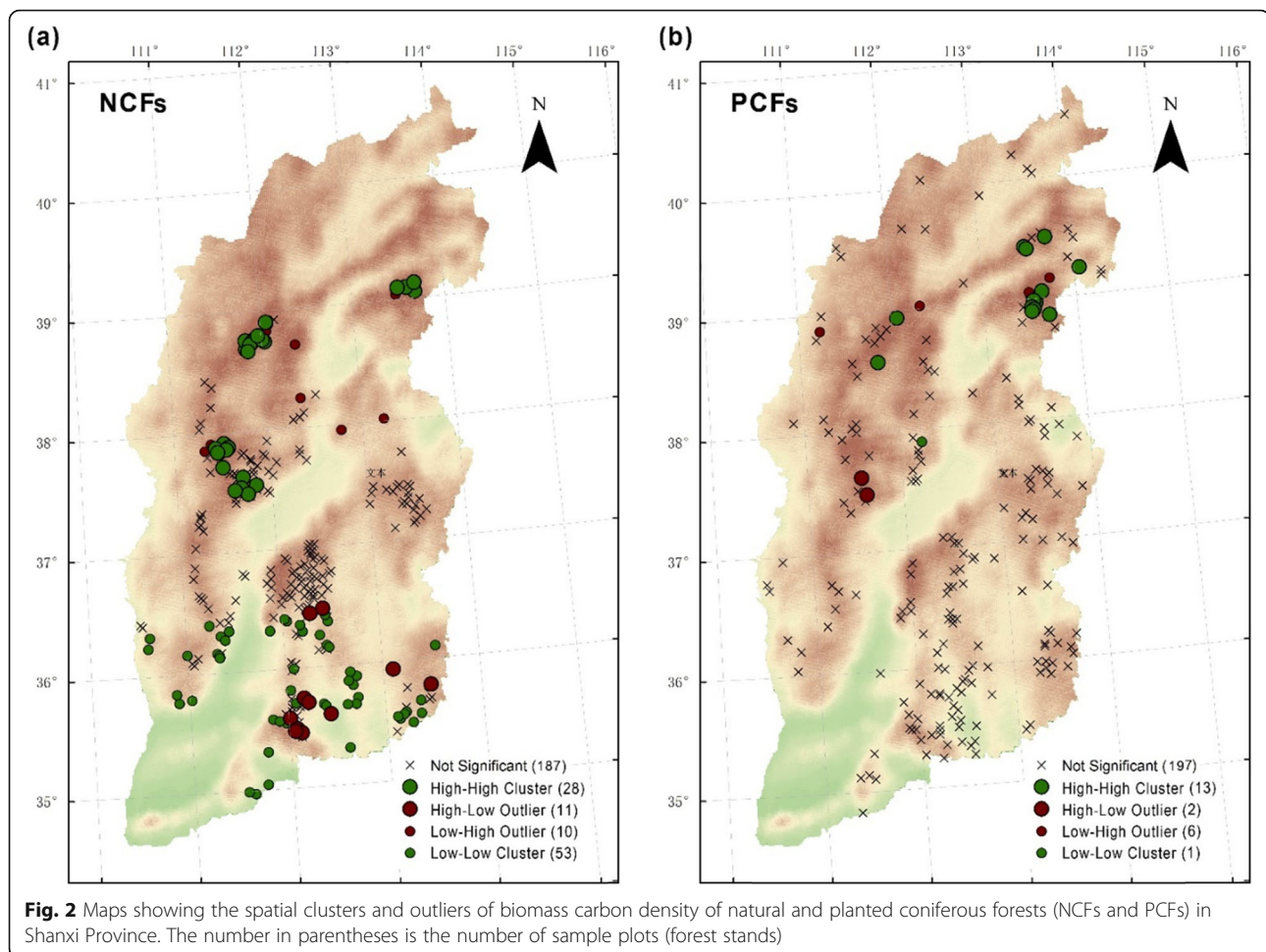
southernmost part of Lüliang Mountains, the southernmost part of Taihang Mountains, the south of Taiyue Mountains and the northeast of Zhongtiao Mountains, while the only one low-low cluster for PCFs was observed in the middle section of Lüliang Mountains. Besides, some high-low outliers were found in the Taiyue, and Zhongtiao Mountains, and the southernmost part of the Taihang Mountains for NCFs, but only two high-low outliers were observed in Guandi Mountain for PCFs. As a whole, the total number of clusters of BCD for NCFs was substantially larger than that for PCFs (81 and 14, respectively), accounting for 28.0% and 6.4% of the forest stands for them, respectively. Noticeably, the high-high and low-low cluster areas of BCD for NCFs were distributed in the north and south mountainous areas of Shanxi, respectively; while both high-high and low-low clusters of BCD for PCFs were distributed in the north mountainous areas of Shanxi.

Moreover, the Getis-ord G^* analysis showed that for NCFs, all the hot-spots of BCD were distributed in the north of 37°N in Shanxi (Fig. 3), including some areas of Luya, Guandi, Wutai and Taihang Mountains, while all the cold-spots of BCD were located in the south of 37°N in the province, including some areas of the southernmost part of Lüliang Mountains, the southernmost part of Taihang Mountains, the south of Taiyue Mountains and the northeast part of Zhongtiao Mountains. In contrast, for PCFs, there were a small number of hot- and cold-spots of BCD that were distributed in the north of 37°N in Shanxi. The hot-spots occurred in some areas of the Wutai, Hengshan and Luya Mountains, and the cold-spots in the middle section of the Taihang Mountains. This suggests that relative to the regional average, the BCD was generally higher in the north but lower in the south for NCFs, while the BCD was only higher or lower in some mountainous areas in the north of 37°N for PCFs over the province. The hot-spot and cold-spot patterns for NCFs and PCFs were in line with the high-high and low-low clusters revealed by Anselin Local Moran's I analysis for them, respectively.

Table 4 Mean biomass carbon density (Mg·ha⁻¹) of individual age groups of natural, and planted coniferous forests in the study region

Forest type	Young		Half-mature		Near-mature		Mature	
	Natural	Planted	Natural	Planted	Natural	Planted	Natural	Planted
<i>Pinus</i>	12.56_a	6.45 _b	24.12_a	17.70 _a	29.29 _a	25.73 _a	28.61 _a	22.47 _a
<i>Platyclusus</i>	6.53 _a	3.44 _a	14.95 _b	11.83 _b	–	–	6.09	–
<i>Larix</i>	12.49 _a	15.59 _b	51.36 _c	35.97 _c	80.29_b	29.37 _a	65.49 _b	39.5 _a
<i>Picea</i>	12.52 _a	39.06 _b	111.97 _d	152.74 _d	76.62 _b	–	–	–
others	0.57	1.69	30.16	–	–	–	–	–
Mean	11.33	6.87	29.28	22.62	34.01	26.07	33.51	25.63

(1) The mean highlighted in bold for natural forests is significantly different from that for planted forests ($P < 0.05$). (2) Within a column, means followed by different letters are significantly different ($P < 0.05$)



Furthermore, semivariogram analysis showed a clear difference in the spatial heterogeneity of biomass carbon density between natural and planted forests (Table 5). The smaller value of nugget-to-sill for natural than for planted forests (0.692 versus 0.887) indicated that the spatial dependence of biomass carbon density was substantially higher for the former than the latter across the entire region. Noticeably, this analysis also showed a much higher spatial dependence of BCD for natural than for planted forests based on the data from the cluster and outlier analysis (sill = 0.5540 and 0.1592, respectively) and the hot spot analysis (sill = 0.6580 and 0.0427, respectively).

Influences of various factors on biomass carbon density

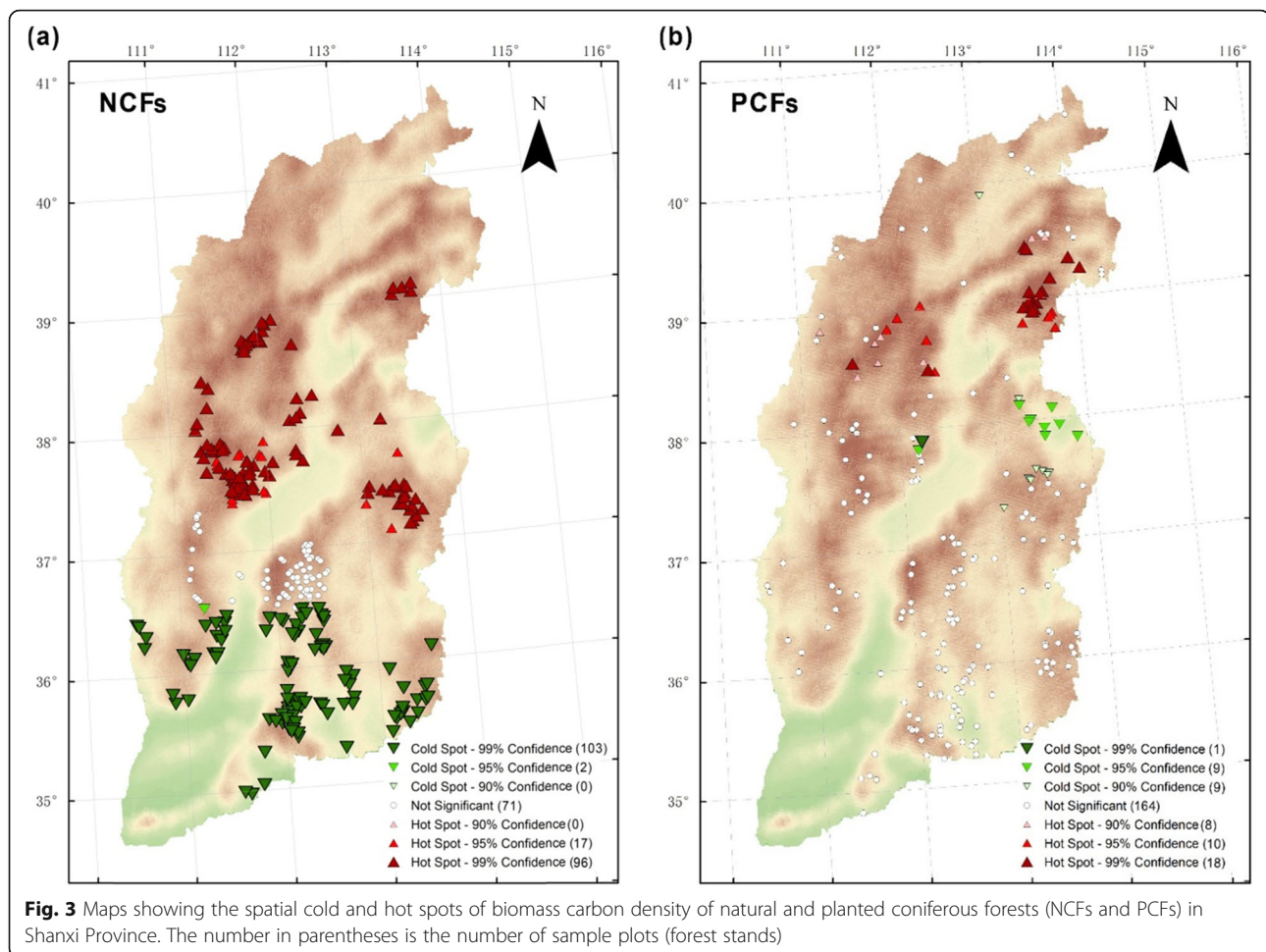
The multi-group SEM model accounted for 56.0% and 57.0% of the variation in BCD for NCFs and PCFs, respectively (Fig. 4). ELE had the greater total effect on BCD than other driving factors for both NCFs and PCFs in Shanxi, with the total effect stronger for NCFs (0.409) than PCFs (0.339). The effects of ELE on BCD included the direct effect and indirect effect by affecting AGE for

both NCFs and PCFs, with direct effect stronger than indirect effect for NCFs (0.348 versus 0.062) and PCFs (0.264 versus 0.076). Meanwhile, AGE, COV and PRCP also showed positive direct effects on BCD, and AGE and PRCP had indirect positive effects by affecting COV. The total effects of the three driving factors decreased in the order: AGE > COV > PRCP for both NCFs and PCFs. Moreover, LAT presented only indirect effects on BCD for NCFs and PCFs (Annex 5 of Additional file 1), with the total effect stronger for NCFs than PCFs. The result of multi-group analysis generally indicated that ELE and AGE were important driving factors of BCD for both NCFs and PCFs. Compared with other factors, the effects of both latitude and elevation on BCD showed much greater difference between NCFs than PCFs.

Discussion

Increasing biomass carbon density and storage

The current study revealed that the BCD was significantly greater for natural than for planted coniferous forests in Shanxi. The higher BCD for the former than the latter can be primarily attributed to the distinct



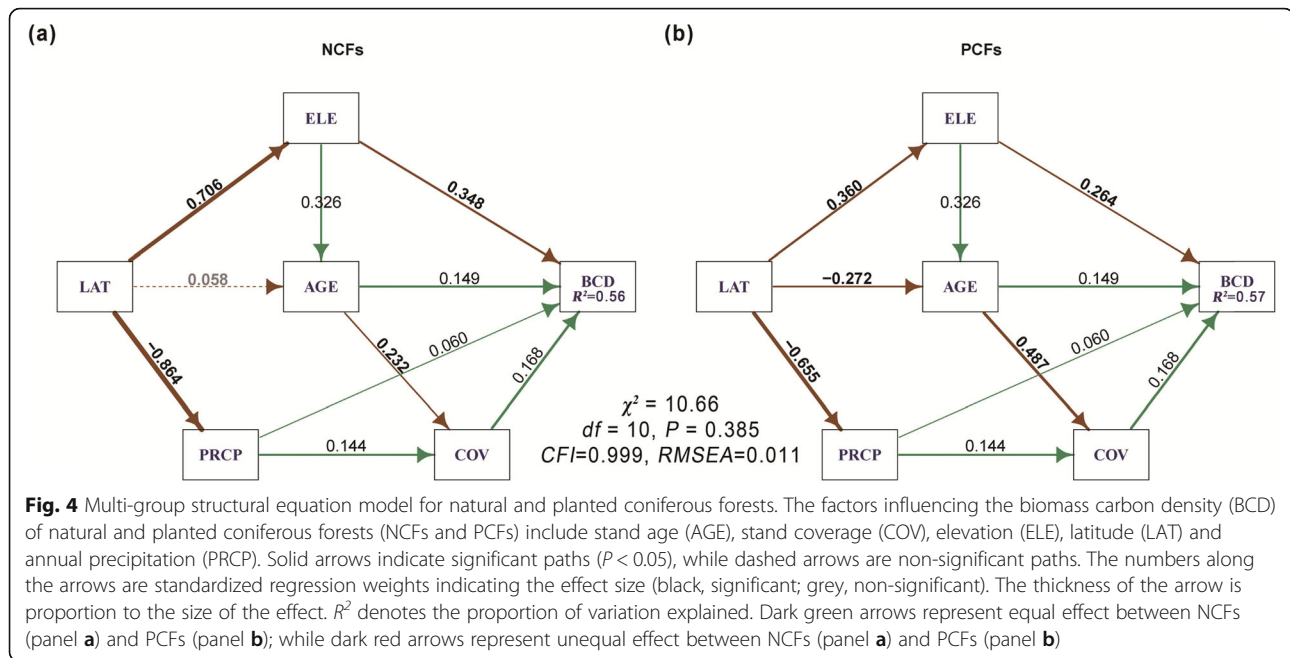
difference in stand age. The stand age for NCFs was nearly twice that for PCFs (at an average age of 54.1 and 28.5 years, respectively). For the largely same reason, the BCD was higher for each type of the natural coniferous forests than for its planted counterparts, because the stand age for the former was at least 1.7 times that for the latter. For example, the huge difference in BCD between natural and planted *Platycladus* forests ($11.74 \text{ Mg}\cdot\text{ha}^{-1}$ versus $1.95 \text{ Mg}\cdot\text{ha}^{-1}$) was obviously related to the larger stand age for natural than for planted *Platycladus* forests (at an average age of 47.9 and 12.9 years, respectively).

Li and Lei (2010) have reported that natural and planted forests accounted for 83.05% and 16.95% of the total carbon stock across China, respectively. In our study, the representative area of a sample plot is 15.8 km^2 , and the total area of natural and planted coniferous forests is 45.50 and 34.46 ha, respectively. The natural and planted coniferous forests accounted for 65.1% and 34.9% of the total carbon stock, respectively (Table 3). The large contribution of planted coniferous forests to the carbon stock was chiefly due to vast changes in land use in past decades. The implementation of the Three-North Shelter Forest Program and the Program for

Table 5 Estimated parameters of semivariogram based on the data of biomass carbon density and from cluster and outlier analysis for natural and planted coniferous forests

Forest type	Data	Model	Nugget (C_0)	Sill ($C_0 + C$)	Nugget effect $C_0/(C_0 + C)$	Range (km)	RSS	R^2
Natural	Biomass carbon density	Exponential	0.2680	0.8710	0.692	57.6	0.0445	0.728
	Cluster and outlier analysis	Gaussian	0.0470	0.5540	0.915	885.1	0.0015	0.915
Planted	Biomass carbon density	Exponential	0.0040	0.0349	0.887	15.3	0.0002	0.022
	Custer and outlier analysis	Exponential	0.0306	0.1592	0.808	2133.0	0.0020	0.591

RSS residual sum of squares; and R^2 , coefficient of determination



Conversion of Cropland into Forests has led to a huge increase in planted coniferous forests. Moreover, because majority of the natural coniferous forests and most of the planted coniferous forests (67.8% and 83.1%, respectively) were at young and half-mature ages under the current inventory, it is expected that the total carbon stock of coniferous forests will increase in future, and that planted coniferous forests will contribute more to future carbon stock in Shanxi.

Spatial patterns of biomass carbon density

The spatial pattern of BCD for NCFs was clearly different from that for PCFs. Although the spatial variation of BCD was related to natural and anthropogenic factors for both NCFs and PCFs, the spatial pattern of BCD for the former was likely shaped to a greater extent by natural influences, while that for the latter was probably formed to a greater extent due to anthropogenic influences. For NCFs, the spatial pattern of BCD was first closely related to the spatial distribution patterns of forest types across the region, and the associated difference in BCD among forest types. As shown in Fig. 1b, most of the natural *Picea* and *Larix* forests are distributed in the north Shanxi, while majority of the natural *Pinus* and *Platycladus* forests are located in the south Shanxi. More important, the BCDs for the former were much higher, while the BCDs for the latter were much smaller compared with the average BCD for NCFs as a whole (Tables 3 and 4). Meanwhile, the establishment of natural reserves for the protection of natural *Picea* and *Larix* forests might have enhanced the formation of the high-high clusters of BCD or hot spots of BCD in the

core areas of natural reserves, where the forests had a continuous distribution and were well protected. On the other hand, the spatial distribution patterns of planted coniferous forests were to great extent different from those of their natural counterparts (Fig. 1b) as a result of reforestation and particularly afforestation. For instance, the planted *Pinus* forests, which accounts for 67.6% of all the planted forests, were distributed across the entire region, at lower elevations generally. Because most of the planted coniferous forests were still at the young and half-mature stages as above mentioned, the BCDs for planted *Pinus* and *Platycladus* forests were generally lower than the average BCD for PCFs as a whole (Tables 3 and 4), and only some of planted *Picea* and *Larix* forests had a higher than average BCD. Therefore, only a small number of the high-high clusters of BCD or hot spots of BCD were identified for planted coniferous forests in the north mountainous areas of Shanxi.

Effect of elevation versus temperature on biomass carbon density

We found that ELE was the most important driving factor of BCD among the five factors tested, and effect of ELE was greater for NCFs than for PCFs. Elevation gradient is associated with changes in temperature and precipitation, and forest type (Sanaei et al. 2018). ELE can affect forest canopy, stem density and stand basal area, and therefore affect aboveground biomass (Xu et al. 2018a, 2018b) through regulating moisture and soil water availability (Fisk et al. 1998). Based on the SEM, Xu et al. (Xu et al. 2018a, 2018b) reported that ELE was the most important abiotic driving factor of vegetation

carbon stocks, while canopy density and forest age were the most crucial driving factors of vegetation carbon stocks in Zhejiang Province, China. The unusually large effect of ELE on BCD for NCFs in Shanxi was probably due to that the range of elevation (483 to 2560 m) over this mountainous region is much larger than that in Zhejiang Province (2 to 1530 m), and noticeably, the *Picea* and *Larix* forests are generally distributed at a higher elevation than *Pinus* and *Platycladus* forests across the entire region (Table 1); and the BCD for the former was generally greater than for the latter, as indicated by the much higher mean BCDs for the former, while much lower mean BCDs for the latter compared with the overall average BCD of natural coniferous forests (Table 4). In addition, the positive correlation of ELE with AGE and COV also enhanced the total positive effect of ELE on BCD. This was probably due to that the forests at higher elevations have usually experienced little disturbance, and can grow steadily and present higher BCD until the mature stage.

However, it was worthy note that we eliminated annual mean temperature (TEMP) in the multi-group SEM because of the collinear relationship between ELE and TEMP, and the stronger correlation of biomass carbon density with ELE than with TEMP (Annex 1 of Additional file 1). To examine further what the result could be if TEMP rather than ELE was selected, we performed the multi-group SEM for NCFs and PCFs again (Fig. 5 and Annexes 3, 6 and 7 of Additional file 1). It was interesting that similar result was found from the analysis except for that the effect of elevation was replaced by the effect of TEMP, which showed a significant direct negative effect on BCD for NCFs and PCFs (Fig. 5). The total effects of the driving factors were -0.367 (TEMP), 0.244 (LAT), 0.200 (AGE), 0.177 (COV) and 0.110 (PRCP) for NCFs; and -0.367 (TEMP), 0.248 (AGE), 0.177 (COV),

0.110 (PRCP) and 0.038 (LAT) for PCFs (Annex 7 of Additional file 1). This result suggested that TEMP could be to great extent taken as an alternative factor to ELE in the multi-group SEM for NCFs and PCFs. The negative effect of TEMP on BCD is consistent with the latest study in the Lüliang Mountains (Wang et al. 2018a).

Effects of other factors on biomass carbon density

AGE and COV were other important factors in modulating the BCD in NCFs and PCFs. The strong positive effect of AGE on BCD could be attributed to cumulative tree growth over time (Ali et al. 2016). Meanwhile, as hypothesized, we found that AGE was significantly positively related to COV, which had a strong direct effect on BCD. Our findings were in agreement with Xu et al. (Xu et al. 2018a, 2018b) who found that canopy density and forest age were the dominant determinants of vegetation carbon density in subtropical forest ecosystems. The pronounced effect of AGE on BCD was a good reflection of the process that the BCD increased with stand age from young to near-mature ages (Annex 4 of Additional file 1). Although the BCD declined slightly at the mature stage, the forests at this stage only accounted for a small proportion of the total forests.

Multi-group SEM revealed that LAT affected BCD indirectly and the total positive effect for NCFs was much greater than that for PCFs. Similarly, Guo and Ren (2014) reported that tree biomass had stronger latitudinal trend in natural forests than in planted forests across China. It was interesting that further analysis showed much stronger correlation, for NCFs than for PCFs, of LAT with the corresponding BCDs derived from Hot spot analysis ($r = 0.893$, $P < 0.001$; $r = 0.361$, $P < 0.001$) and Clusters and Outliers analysis ($r = 0.543$, $P < 0.001$; $r = 0.215$, $P = 0.001$). This implied that the relationship between LAT and BCD detected

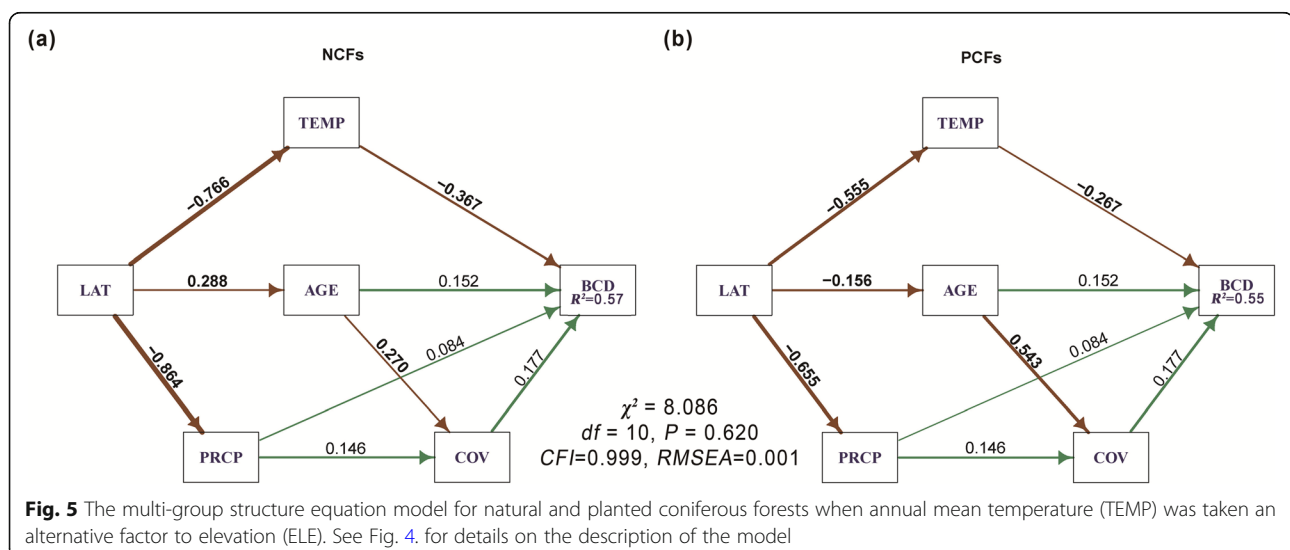


Fig. 5 The multi-group structure equation model for natural and planted coniferous forests when annual mean temperature (TEMP) was taken an alternative factor to elevation (ELE). See Fig. 4. for details on the description of the model

by multi-group SEM well reflected the spatial pattern of BCDs for NCFs and PCFs.

Different from the previous studies in which the relationships of latitude and other factors with vegetation carbon density were analyzed separately (Guo and Ren 2014; Wen and He 2016), our study incorporated LAT into SEM to assess the indirect effects of LAT via other driving factors. In this way, we found that the final total indirect effect of LAT on BCD was the combined effects of LAT on ELE, AGE and PRCP (Fig. 4). Therefore, the introduction of LAT into SEM could help us to understand the mechanism of effect of LAT on BCD. Noticeably, we found that the difference in the total effect of LAT between NCFs and PCFs was mainly due to the different effect of LAT on ELE and AGE (Fig. 4). The stronger positive effect of LAT on BCD for NCFs than PCFs was due to the larger positive effect of LAT on ELE for the former than the latter and no effect of LAT on AGE for NCFs but a large negative effect on AGE for PCFs. The larger difference in the effect of LAT on BCD between NCFs and PCFs was to some extent a mirror of the difference in the spatial patterns of BCDs between these two types of forests in the study region.

Conclusions

The present study found that the biomass carbon density and carbon stock were significantly greater for natural than planted coniferous forests in Shanxi. However, the planted coniferous forests will contribute more to future total carbon stock. Spatially, the higher biomass carbon density for the two forest types was clustered in the north mountainous areas, and the clustered number was larger for natural than planted coniferous forests. Meanwhile, the biomass carbon density of only natural coniferous forests was detected the clustered area in the south mountainous areas. Obviously, a much higher spatial dependence of biomass carbon density for natural than for planted forests. The effect of each driving factor on biomass carbon density was not always consistent between forest types. Elevation was the most important driving factor, and the effect on biomass carbon density was stronger for natural than planted coniferous forests. Latitude presented only indirect effects on biomass carbon density, and the difference between the two forest types was to some extent a mirror of the difference in the spatial patterns of BCDs between them in the study region.

Supplementary information

Supplementary information accompanies this paper at <https://doi.org/10.1186/s40663-020-0218-7>.

Additional file 1: Annex 1. More information on multi-group SEM. **Annex 2.** The priori (a) and good-fitting (b) structure equation models showing the factors that have direct and indirect effects on biomass

carbon density of coniferous forests in Shanxi, China. **Annex 3** The priori (a) and good-fitting (b) structure equation models showing the factors that have direct and indirect effects on biomass carbon density of coniferous forests in Shanxi, China. **Annex 4** Biomass carbon storage (BCS) of individual age groups of natural, planted and all coniferous forests in the study region. **Annex 5** Direct, indirect and total effects of stand age (AGE), stand coverage (COV), elevation (ELE), latitude (LAT) and annual mean precipitation (PRCP) on biomass carbon density (BCD) for natural and planted coniferous forests and for all coniferous forests. **Annex 6** Multi-group comparison of path coefficients between forest types. A non-significant value, highlighted in bold, indicates that the path contribution to the model is equal between forest types. **Annex 7** Direct, indirect and total effects of stand age (AGE), stand coverage (COV), latitude (LAT), annual mean temperature (TEMP) and annual mean precipitation (PRCP) on biomass carbon density (BCD) for natural and planted coniferous forests and for all coniferous forests.

Abbreviations

BCD: Biomass carbon density; COV: Stand coverage; ELE: Elevation; LAT: Latitude; NCFs: Natural coniferous forest; PCFs: Planted coniferous forests; PRCP: Mean annual precipitation; SEM: Structural equation modeling; TEMP: Annual mean temperature

Acknowledgments

We acknowledge the Carbon Sequestration Monitoring Center of Forestry Investigation and Planning Institute in Shanxi for providing us national forest inventory data as well as useful advices for their manipulation.

Authors' contributions

Conceived and designed the study: SL, WM and FX. Analyzed the data: SL and FX. Wrote the paper: SL, WM and FX. All authors read and approved the final manuscript.

Funding

This work was supported by the Shanxi Province Science and Technology Project (Grant number: 2014091003–0106).

Availability of data and materials

The dataset used and/or analyzed during the current study are available from the corresponding author on reasonable request.

Ethics approval and consent to participate

Not applicable.

Competing interests

The authors declare that they have no competing interests.

Received: 2 August 2019 Accepted: 22 January 2020

Published online: 06 February 2020

References

- Ali A, Yan E-R, Chen HYH, Chang SX, Zhao YT, Yang XD, Xu MS (2016) Stand structural diversity rather than species diversity enhances aboveground carbon storage in secondary subtropical forests in eastern China. *Biogeosciences* 13:4627–4635. <https://doi.org/10.5194/bg-13-4627-2016>
- Bollen KA (1989) *Structural equations with latent variables*, 1st edn. Wiley-Interscience, New York
- Chang R, Wang G, Fei R, Yang Y, Luo J, Fan JR (2015) Altitudinal change in distribution of soil carbon and nitrogen in Tibetan montane forests. *Soil Sci Soc Am J* 79. <https://doi.org/10.2136/sssaj2015.02.0055>
- Cheng X, Han H, Kang F (2012) Biomass, carbon accumulation and its partitioning of a *Pinus tabulaeformis* plantation ecosystem in Shanxi Province, China. *Chinese J Ecol* 31:2455–2460 (in Chinese)
- Chi L, Wang B, Cao X, Wang N, Wang W, Wang R, Yang H (2014) Carbon storage of Chinese pine forest ecosystem in the Central Shanxi Province. *J Arid Land Res Environ* 28:81–84 (in Chinese)
- Dai W, Fu WJ, Jiang PK, Zhao KL, Li YH, Tao JX (2018) Spatial pattern of carbon stocks in forest ecosystems of a typical subtropical region of southeastern China. *Forest Ecol Manag* 409:288–297. <https://doi.org/10.1016/j.foreco.2017.11.036>

- Durán SM, Sánchez-Azofeifa GA, Rios RS, Gianoli E (2015) The relative importance of climate, stand variables and liana abundance for carbon storage in tropical forests: climate, stand variables and lianas control forest carbon. *Glob Ecol Biogeogr* 24:939–949
- Editorial Board of Forests in Shanxi (1992) *Forests in Shanxi* (in Chinese). China Forestry Publishing House, Beijing
- Eldery AA, Garcia LA (2010) Comparison of ordinary Kriging, regression Kriging, and Cokriging techniques to estimate soil salinity using Landsat images. *J Irrig Drain Engineer* 136(6):355–364. [https://doi.org/10.1061/\(ASCE\)IR.1943-4774.0000208](https://doi.org/10.1061/(ASCE)IR.1943-4774.0000208)
- Fan X, Wang M (2011) Change trends of air temperature and precipitation over Shanxi Province, China. *Theor Appl Climatol* 103:519–531
- Fang J (2001) Changes in forest biomass carbon storage in China between 1949 and 1998. *Science* 292:2320–2322. <https://doi.org/10.1126/science.1058629>
- FAO (2010) Global forest resources assessments. <http://www.fao.org/forest-resources-assessment/past-assessments/fra-2010/en/>. Accessed 4 Jun 2019
- FAO (2015) Global forest resources assessments. <http://www.fao.org/forest-resources-assessment/past-assessments/fra-2015/en/>. Accessed 4 Jun 2019
- Fisk MC, Schmidt SK, Seastedt TR (1998) Topographic patterns of above- and belowground production and nitrogen cycling in alpine tundra. *Ecology* 79: 2253–2266
- Fu WJ, Fu ZJ, Ge HL, Ji BY, Jiang PK, Li YF, Wu JS, Zhao KL (2015) Spatial variation of biomass carbon density in a subtropical region of southeastern China. *Forests* 6:1966–1981
- Fu WJ, Jiang PK, Zhou GM, Zhao KL (2014) Using Moran's I and GIS to study the spatial pattern of forest litter carbon density in a subtropical region of southeastern China. *Biogeosciences* 11:2401–2409. <https://doi.org/10.5194/bg-11-2401-2014>
- Gairola S, Sharma CM, Ghildiyal SK, Suyal S (2011) Live tree biomass and carbon variation along an altitudinal gradient in moist temperate valley slopes of the Garhwal Himalaya (India). *Curr Sci India* 100:1862–1870
- Grace JB, Anderson TM, Olff H, Scheiner SM (2010) On the specification of structural equation models for ecological systems. *Ecol Monogr* 80:67–87
- Guo M, Liu Y, An W, Liu W, Li Z, Yan J (2015) *Shanxi Climate*. China Meteorological Press, Beijing (in Chinese)
- Guo Q, Ren H (2014) Productivity as related to diversity and age in planted versus natural forests. *Glob Ecol Biogeogr* 23:1461–1471
- Lamsal S, Cobb RC, Hall Cushman J, Meng Q, Rizzo D, Meentemeyer RK (2011) Spatial estimation of the density and carbon content of host populations for *Phytophthora ramorum* in California and Oregon. *Forest Ecol Manag* 262:989–998. <https://doi.org/10.1016/j.foreco.2011.05.033>
- Law BE, Sun OJ, Campbell J, Van Tuyl S, Thornton PE (2003) Changes in carbon storage and fluxes in a chronosequence of ponderosa pine. *Glob Chang Biol* 9:510–524. <https://doi.org/10.1046/j.1365-2486.2003.00624.x>
- Li H, Lei Y (2010) Estimation and Evaluation of Forest Biomass Carbon Storage in China (in Chinese). China Forestry Publishing House, Beijing, China.
- Lin Z, Chao L, Wu C, Hong W, Hong T, Hu X (2017) Spatial analysis of carbon storage density of mid-subtropical forests using geostatistics: a case study in Jiangle County, Southeast China. *Acta Geochim* 37:90–101. <https://doi.org/10.1007/s11631-017-0160-8>
- Liu N, Nan H (2018) Carbon stocks of three secondary coniferous forests along an altitudinal gradient on loess plateau in inland China. *PLoS One* 13:e0196927. <https://doi.org/10.1371/journal.pone.0196927>
- Liu Y, Yu G, Wang Q, Zhang Y (2014) How temperature, precipitation and stand age control the biomass carbon density of global mature forests. *Global Ecol Biogeogr* 23:323–333. <https://doi.org/10.1111/gbi.12186>
- Ma Z (2001) *Vegetation of Shanxi Province*. China science and technology press. Beijing, China (in Chinese)
- Manepalli URR, Bham GH, Kandada S (2011) Evaluation of hot-spots identification using Kernel density estimation and Getis-ord on I-630. <https://trid.trb.org/view/1286977>. Accessed 4 Jun 2019
- Pan YD, Birdsey RA, Fang JY, Houghton R, Kauppi PE, Kurz WA, Phillips OL, Shvidenko A, Lewis SL, Canadell JG, Ciais P, Jackson RB, Pacala SW, McGuire AD, Piao SL, Rautiainen A, Sitch S, Hayes D (2011) A large and persistent carbon sink in the world's forests. *Science* 333:988–993. <https://doi.org/10.1126/science.1201609>
- Plouffe CCF, Robertson C, Chandrapala L (2015) Comparing interpolation techniques for monthly rainfall mapping using multiple evaluation criteria and auxiliary data sources: a case study of Sri Lanka. *Environ Model Softw* 67: 57–71. <https://doi.org/10.1016/j.envsoft.2015.01.011>
- Price MF, Butt N, International Union of Forestry Research Organizations (eds) (2000) *Forests in Sustainable Mountain development: a state of knowledge report for 2000*. CABI pub. association with the International Union of Forestry Research Organizations, Wallingford, Oxon, UK; New York, NY, USA
- Ren H, Chen H, Li L, Li P, Hou C, Wan H, Zhang Q, Zhang P (2013) Spatial and temporal patterns of carbon storage from 1992 to 2002 in forest ecosystems in Guangdong, southern China. *Plant Soil* 363:123–138. <https://doi.org/10.1007/s11104-012-1302-8>
- Robertson GP (1987) Geostatistics in ecology: interpolating with known variance. *Ecology* 68:744–748. <https://doi.org/10.2307/1938482>
- Rosseel Y (2012) Lavaan: An R package for structural equation modeling. *J stat soft*. <https://doi.org/10.18637/jss.v048.i02>
- Rossi RE, Mulla DJ, Journel AG, Franz EH (1992) Geostatistical tools for modeling and interpreting ecological spatial dependence. *Ecol Monogr* 62:277–314. <https://doi.org/10.2307/2937096>
- Sanaei A, Chahouki MAZ, Ali A, Jafari M, Azarnivand H (2018) Abiotic and biotic drivers of aboveground biomass in semi-steppe rangelands. *Sci Total Environ* 615:895–905. <https://doi.org/10.1016/j.scitotenv.2017.10.010>
- Shipley B (2004) Cause and correlation in biology: a User's guide to path analysis, structural equations and causal inference, Nachdr. Cambridge University Press, Cambridge
- Sun J (2011) Study on biomass and carbon stock in *Pinus Tabulaeformis* plantation of Taiyue Mountain. Beijing Forestry University, Beijing, China (in Chinese)
- Verkerk PJ, Fitzgerald JB, Datta P, Dees M, Hengeveld GM, Lindner M, Zudin S (2019) Spatial distribution of the potential forest biomass availability in Europe. *For Ecosyst* 6(1):5. <https://doi.org/10.1186/s40663-019-0163-5>
- Wang N, Wang B, Wang R, Cao X, Wang W, Chi L (2014a) Density and distribution patterns of carbon of *Pinus tabulaeformis* Carr. Forest ecosystem in Shanxi Province, China. *J Basic Sci Eng* 22:58–68 (in Chinese)
- Wang QX, Fan XH, Wang MB (2014b) Recent warming amplification over high elevation regions across the globe. *Clim Dyn* 43:87–101. <https://doi.org/10.1007/s00382-013-1889-3>
- Wang Y, Wang Q, Wang M (2018a) Similar carbon density of natural and planted forests in the Lüliang Mountains, China. *Ann Forest Sci* 75. <https://doi.org/10.1007/s13595-018-0753-3>
- Wang Y, Wang Q, Wang M (2018b) Basic parameters for estimating the volume, biomass and carbon density of the main dominant tree species (species groups) in the Lüliang Mountains, China. <http://hts.sxu.edu.cn/sxssts/jpt/index.htm>. Accessed 4 Jun 2019 (in Chinese)
- Wang Z (1999) *Geostatistics and its application in ecology*. Science Press, Beijing, China (in Chinese)
- Wen D, He N (2016) Forest carbon storage along the north-south transect of eastern China: spatial patterns, allocation, and influencing factors. *Ecol Indic* 61:960–967. <https://doi.org/10.1016/j.ecolind.2015.10.054>
- Xiao X (2005) *National Forest Inventory of China*. China Forestry Publishing House, Beijing, China (in Chinese)
- Xu B, Guo ZD, Piao SL, Fang JY (2010) Biomass carbon stocks in China's forests between 2000 and 2050: a prediction based on forest biomass-age relationships. *Sci China Life Sci* 53:776–783. <https://doi.org/10.1007/s11427-010-4030-4>
- Xu L, Shi Y, Fang H, Zhou G, Xu X, Zhou Y, Tao J, Ji B, Xu J, Li C, Chen L (2018a) Vegetation carbon stocks driven by canopy density and forest age in subtropical forest ecosystems. *Sci Total Environ* 631–632:619–626. <https://doi.org/10.1016/j.scitotenv.2018.03.080>
- Xu M, Ji H, Zhuang S (2018b) Carbon stock of Moso bamboo (*Phyllostachys pubescens*) forests along a latitude gradient in the subtropical region of China. *PLoS One* 13:e0193024. <https://doi.org/10.1371/journal.pone.0193024>
- Zald HSJ, Spies TA, Seidl R, Pabst RJ, Olsen KA, Steel EA (2016) Complex mountain terrain and disturbance history drive variation in forest aboveground live carbon density in the western Oregon cascades, USA. *Forest Ecol Manag* 366:193–207. <https://doi.org/10.1016/j.foreco.2016.01.036>